agriculture

Article

Development of a Cereal–Legume Intercrop Model for DSSAT Version 4.8

Jacques Fils Pierre [1], Upendra Singh [1], Esaú Ruiz-Sánchez [2] and Willingthon Pavan [1,*]

[1] International Fertilizer Development Center, Muscle Shoals, AL 35662, USA; usingh@ifdc.org (U.S.); jpierre@ifdc.org (J.F.P.)
[2] Division of Postgraduate Studies and Research, Tecnológico Nacional de México, Campus Conkal, Conkal 973453, Mexico; esau.ruiz@itconkal.edu.mx
* Correspondence: wpavan@ifdc.org; Tel.:+1-256-381-6600

Abstract: Intercropping is extensively used to increase land productivity and agricultural benefits. In developing countries, intercropping has historically been one of the most widely used cropping systems. Crop models have been used to assess risk productivity over time and space, particularly in monocropping systems. Crop models, such as the Decision Support System for Agrotechnology Transfer (DSSAT), have been widely used to improve crop growth, development, and yield predictions; however, this model has some limitations when assessing interspecific competition in intercropping systems (e.g., it does not have a subroutine capable of running two crops simultaneously). Therefore, in this study, we developed a new approach to allow DSSAT to run two crop species in intercropping systems. A light interception algorithm and modified source code were integrated into the DSSAT to simulate the relay-strip intercropping system. The intercrop model developed in this study is the first intercrop model for DSSAT. This model is generic and can be employed to build other cereal–legume intercrop models for DSSAT Version 4.8. Regarding risk assessment of crop production, the model can evaluate long-term cereal–legume intercrop yields in low-input cropping systems. Therefore, before officially launching the new model in DSSAT, more field trials are recommended to rigorously evaluate and improve the model with data from different environments. The intercrop model developed in this study is simple, so this modeling approach can be employed to develop other cereal–noncereal intercrop models.

Keywords: cowpea; crop model; intercropping systems; light interception; maize

Citation: Pierre, J.F.; Singh, U.; Ruiz-Sánchez, E.; Pavan, W. Development of a Cereal–Legume Intercrop Model for DSSAT Version 4.8. *Agriculture* **2023**, *13*, 845. https://doi.org/10.3390/agriculture13040845

Academic Editors: Rabin Bhattarai and Hamze Dokoohaki

Received: 11 March 2023
Revised: 1 April 2023
Accepted: 5 April 2023
Published: 10 April 2023

1. Introduction

Intercropping cereals and legumes is becoming increasingly popular in tropical regions [1–4], allowing for two or more crops to be grown in the same field during the same growing season [5–7]. In the traditional cropping system of the Yucatan Peninsula, C4 cereal crops, such as maize (*Zea mays* L.), are the dominant crop species, while C3 legume crops, such as lima bean (*Phaseolus lunatus* L.) and cowpea (*Vigna unguiculata* L. Walp) are the most common associated species used by growers [6]. Squash (*Cucurbita* spp.) is also part of the traditional cropping system of the region. Among its multiple benefits, this practice captures more radiation, makes better use of available water and nutrients, reduces pest and disease incidence, and suppresses weeds [8–10]. However, there is more competition for water, nutrients, light, and space in intercropping systems than in monocropping systems. In most cereal–legume intercropping, the cereal often has a taller canopy and deeper roots than the legume species, leading to a more efficient use of resources by cereals [11,12]. Many studies have found a link between the amount of radiant energy captured and the number of crops grown [13,14].

As maize is the dominant crop in an intercropping system, the available water and nutrients are shared between the two species [15]. The performance of both crops is influenced by environmental and socioeconomic factors, crop management, and germplasm [16,17].

Although strategies such as optimal fertilizer application and delayed legume planting can improve system performance, their design in an intercropping system can be time-consuming and expensive. Therefore, models can facilitate collaboration between decision makers and researchers, saving time and money [18,19].

Several intercrop models simulate light competition, but most intercrop models assume that the canopy is the same all the way across [18,19]. However, in intercropping systems, light competition depends on planting configuration (row spacing, sowing densities, and sowing dates). Border row effects are also crucial in such systems [20]. Developing a model-based decision support system for intercrops could help address low crop productivity, competition, climate change, and soil fertility depletion.

Various models have attempted to deal with intercropping and interspecific competition between two intercropped species [21–24], but few crop growth models have been developed, calibrated, and validated to accommodate the interspecific plant–plant interactions that are important in intercrop performance. Most models do not account for understory species' adaptability. For instance, the Agricultural Production Systems sIMulator (APSIM) does not take into account how shorter intercrop plants respond to shade [24]. Crop modeling software, such as the Decision Support System for Agrotechnology Transfer (DSSAT), APSIM, and the Cropping Systems Simulation Model (CropSyst), simulate crop growth and environmental interactions in various weather and soil conditions [25,26]. Few crop models simulate polyculture well [27,28]. DSSAT is a decision support system for evaluating agricultural management options [20,29]. This suite of models is accurate. DSSAT is a decision support system that accurately simulates crop growth and yield in various crops, including row crops and horticultural crops [29–33]. Nonetheless, DSSAT does not have a specific module that can take into account the overall interspecific competition in mixed cropping systems [17], limiting its use to competition for solar radiation, like most intercropping models [17,34]. Therefore, more generalized models that can account for interspecific competition in an intercropping system are required (i.e., a more general algorithm is needed to take into consideration the fact that crop roots can absorb more water and nutrients). Due to the limited ability of current DSSAT models to deal with uncertainties in intercropping systems, a new intercrop model could be an alternative to deal with interspecific competition (i.e., light competition) in low-input cropping systems, particularly in developing countries. Therefore, the overall goal of this research was to develop and integrate the cereal–legume intercrop model into DSSAT for field applications. This model will help us understand how much light each crop species takes in and how their niches change over time. It is the first DSSAT intercrop module to run two crops simultaneously to simulate development, crop growth, and yield. The intercrop model developed in this study is simple, so this modeling approach can be employed to develop other cereal–noncereal intercrop models. Additionally, detailed model input data and experiment data for calibration and validation are recommended before launching the official version for field applications.

2. Materials and Methods

2.1. MPI_Maize–Legume Intercrop Development

2.1.1. Description of the Intercrop Model

For the model approach, the DSSAT-Cropping System Model (CSM) Version 4.8 software was used, and therein, Crop Environment Resource Synthesis (CERES; i.e., a simulation model of maize growth and development) and CROPGRO (i.e., a generic crop model based on the SOYGRO, PNUTGRO, and BEANGRO models), which were developed for sole cropping systems only, were applied [19,35,36]. DSSAT is a process-oriented crop model that considers soil, plants, atmosphere, and management systems. It was designed to help researchers adapt and test the cropping system model itself as well as for management applications [19]. As the DSSAT model does not account for a module capable of running two crops at the same time [19], a few changes were made to the DSSAT Cropping System Model (CSM) source code so that simulations of two crops in intercropping systems could be run at the same time. The model looks at a cereal and a legume species planted in relay-strip intercropping systems. The intercrop implementation in this study is very simple: it only considers competition for light between both crop species. This implementation is very generic: it can be used for any cereal and legume crop. However, in this study, data from a maize–cowpea field experiment were used to develop the model. Different equations were integrated into the CERES-Maize and CROPGRO models to account for the light competition effect for each crop species. The goal of this integration was to simulate the biomass production and yield of both species in a cereal–legume intercropping system. In this intercrop model, the approach used in DSSAT is maintained to make it easy for anyone to use by evaluating a minimum data set, easily collected in a field (leaf area index [LAI], temperature, solar radiation, soil nitrate and ammonium per layer, bulk density and soil water content per layer, crop phenology, plant population density, and row spacing).

2.1.2. MPI_Maize–Cowpea Intercrop Design Approach

To allow DSSAT to simulate maize–legume intercropping systems, we redesigned the DSSAT module structure using a communication-based approach for a crop model. Lazaretti et al. [36] used a similar method, in which a communication-based approach was used to run a crop model and a plant disease model concurrently while exchanging data through an intermediate relational database management system. In this study, Message Passing Interface (MPI) was used to allow the different models to communicate with each other.

MPI can be defined as a message-passing library or a standardized set of libraries for parallel and high-performance computing (HPC), consisting of exchanging messages between processes. MPI has a protocol with specifications and definitions for resource optimization, defining an abstract application programming interface (API) that allows independent and compatible implementations. Due to the portability and availability of libraries for different languages, such as C/C^{++}, FORTRAN, and Java, MPI was quickly adopted as the standard for executing numerical software in HPC architectures [37]. It is frequently used as a communication switch, where applications can be written in different programming languages and easily communicate with each other, sharing information through a communicator or interface. In this way, MPI shows up as an independent and efficient application to exchange information [38]. A parallel MPI technique was developed for an agroecosystem model, Environmental Policy Integrated Climate (EPIC), on global food and bioenergy studies [39].

The execution using the multiple instruction multiple data (MIMD) implementation criterion allows the same approach to be used for coupling simulation models in parallel. The coupling of different simulation models requires time control, data communication, and synchronization. In this case, the development of a coupling interface simplified its use and implementation in the simulation model [40].

The coupling interface manages the data communication and synchronization of the coupled simulation models. The purpose of the interface is to provide a set of reusable, portable standard features between different programming languages and to simplify the communication of the simulation models [40]. The implementation should include methods that abstract the communication layer with MPI, so the coupling interface works as an independent module. These functions are used at the coupling point of the simulation model, enabling access to the initialization, communication, and finalization routines [38,41].

2.2. Changes Implemented in the DSSAT to Simulate Maize–Cowpea Intercrop

Fraction of Radiation Intercepted

A light interception model modified from a strip-planted crop model [42,43] was applied to calculate the daily fraction of light interception of each species in the strip intercrop. Five different phases were distinguished according to the plant height difference between maize and cowpea, and the fraction of light interception was calculated separately for each phase. Using this strip canopy model, Gou et al. [43] captured the effects of row configurations on light competition. In phases I and IV, only one crop is present, and Equation (1) is used to calculate the fraction of light interception. The radiation interception in a relay strip intercropping system is estimated as a weighted average of a fully compressed canopy (w) and the radiation interception by a homogeneous canopy (1 − w) [42,44]. Thus, in this study, the fraction of radiation intercepted in a strip canopy was calculated using the following equation:

$$f_{strip = f_{homog}(1-w)+f_{compr}w} \tag{1}$$

where f_{strip} is the fraction of radiation intercepted in a strip canopy; f_{homog} is the fraction of light interception by a homogeneous canopy; f_{compr} is the fraction of light interception by this compressed canopy; and w is the weighting factor.

The light interception by a canopy of a homogeneous crop is described using Beer's Law [45]. The fraction of light interception by a homogeneous canopy (f_{homog}) is calculated as

$$f_{homog} = 1 - \exp(-\mathrm{KLAI}) \tag{2}$$

The fraction of light interception by this compressed canopy $\left(f_{compr}\right)$, considering the total land area, is

$$f_{compr} = \left(1 - \exp\left(-kLAI_{compr}\right)\frac{R}{R+P}\right. \tag{3}$$

The leaf area index (LAI) of a compressed canopy (LAI_{compr}) is defined by

$$LAI_{compr} = LAI\frac{R+P}{R} \tag{4}$$

where R is the strip width and P is the width of the path between strips.

The weighting factor w in Equation (1), which represents the relative contribution of the homogeneous and compressed parts, is defined by

$$w = \frac{SP - SR}{1 - \exp\left(-kLAI_{compr}\right)} \tag{5}$$

where SP is the fraction of radiation transmitted to the soil surface in the path and SR is the fraction of radiation transmitted to the soil surface under the strip.

SP and SR are calculated by separating radiation that reaches the soil surface directly from radiation that passes through the leaf canopy. Therefore, the fraction of radiation reaching the path between strips of soil is calculated as follows:

$$SP = IP + (1 - IP)\exp(-kLAI) \tag{6}$$

The fraction of radiation reaching the soil under the strips:

$$SR = IR \times \exp\left(-\mathrm{k}LAI_{compr}\right) + (1 - IR)\exp(-kLAI) \tag{7}$$

IP is the fraction that represents the spatial integration of radiation reaching the path between strips, and IR is the fraction that represents the spatial integration of the radiation reaching the strip [44]. IP is the spatial integral of incoming radiation over the path, assuming a spherical distribution of the angle of the incoming light beam [44]. IP is calculated as follows:

$$IP = \frac{\sqrt{H^2 + P^2 -}\ H}{P} \tag{8}$$

IR is the light interception measured in the strip, resulting from an opaque ("black") crop strip with height H and width W, at a path width P:

$$IR = \frac{\sqrt{H^2 + R^2 -}\ H}{R} \tag{9}$$

The leaf area of the taller crop (maize or cowpea) is subdivided into two parts:

$$LAI_{tp-upper} = \left(1 - \frac{H_{sh}}{H_{tp}}\right) \times LAI_{tp} \tag{10}$$

$$LAI_{tp-lower} = \left(\frac{H_{sh}}{H_{tp}}\right) \times LAI_{tp} \tag{11}$$

In phases II and IV, one crop is taller than the other. In these cases, the canopy is divided into two layers (an upper and lower layer). The upper layer is from the top of the canopy of the taller crop species to the top of the canopy of the shorter species, while the lower layer consists of alternate strips of the two species. Therefore, the fraction of light intercepted by taller crops is subdivided into two parts:

$$f_{taller} = f_{tallerup} + f_{tallerlow} \tag{12}$$

The fraction of light intercepted by the upper part of the taller crop:

$$f_{tp-upper} = f_{\text{homog}-tp-upper} \times \left(1 - W_{tp-upper}\right) + \left(f_{compr-tp-upper \times W_{tp-upper}}\right) \tag{13}$$

Calculations for the upper layer were performed using the model for a strip-planted canopy (Equations (1)–(9)), using the plant height difference of two crops ($H_{tp} - H_{sh}$) and the leaf area index of the upper layer of the taller crop ($LAI_{tp-upper}$) as inputs.

$$F_{homog-tg-upper} = 1 - \exp\left(-k_{tp-upper} LAI_{tp-upper}\right) \tag{14}$$

where $LAI_{tp-upper}$ is the leaf area index of the upper layer of the taller crop.

$$LAI_{cpr-tpr-upper} = LAI_{tp-upper} \times \frac{R+P}{R} \tag{15}$$

where $LAI_{cpr-tp-upper}$ is the compressed leaf area index for the upper layer of the taller crop.

$$F_{cpr-tp-upper} = 1 - \exp\left(-k_{tpr-upperLAI_{cpr-tp-upper}}\right) \times \frac{R}{R+P} \tag{16}$$

where $F_{cpr-tp-upper}$ is the fraction of light interception of the compressed canopy for the upper layer of the taller crop.

The weighting factor w in the following equation, which represents the relative contribution of the homogeneous and compressed parts in the upper part of the taller crop, is defined by

$$w = \frac{SP_{tp-UP} - SR_{Ttp-up}}{1 - \exp\left(-k_{tp-up} LAI_{compr-tp-up}\right)} \tag{17}$$

$$SP_{tp-up} = IP_{tp-up} + \left(1 - IP_{tp-up}\right) \exp\left(-k_{tp-up} LAI_{tp-up}\right) \tag{18}$$

$$SR_{tp-up} = IP_{tp-up} \times \exp\left(-k_{tp-up} LAI_{compr-tp-up}\right) + \left(1 - IR_{tp-up}\right) \exp\left(-k_{tp-up} LAI_{tp-up}\right) \tag{19}$$

IP_{tp-up} and IR_{tp-up} are calculated as follows:

$$IP_{tp-up} = \frac{\sqrt{H_{diff}{}^2 + P^2 -}\ H_{diff}}{P} \tag{20}$$

$$IR_{tp-up} = \frac{\sqrt{H_{diff}{}^2 + R^2 -}\ H_{diff}}{R} \tag{21}$$

$$H_{diff} = H_{tp} - H_{sh} \tag{22}$$

The fraction of light interception by the lower layer of the taller crop was thus calculated as

$$f_{tp-lower} = SR_{tp-lower} \times (1 - \exp\left(-k_{tp}LAI_{tp-lower-cpr}\right) \times \frac{R_{tp}}{R_{tp} + P_{tp}} \tag{23}$$

The fraction of light interception of the shorter crop was calculated, similar to Equation (4), as

$$f_{\text{sh}} = SP_{tp-upper}(1 - \exp(-k_{\text{sh}}LAI_{\text{sh}-cpr}) \times \frac{R_{\text{sh}}}{R_{\text{sh}} + P_{\text{sh}}} \tag{24}$$

In phase III, in the case of intercropping species with equal heights, the fraction of radiation intercepted by each plant strip is calculated according to Equations (12)–(22) as used for phases II and IV, but with *IP* = *IR* = 1 for both species, and *SP* = 1.

2.3. MPI_DSSAT Application to Maize–Legume Intercrop Modeling

Modeling Workflow

In order to test the MPI_DSSAT intercrop implementation, we used data collected from a previous study conducted during the summer and autumn of 2021 in Becal, Campeche, Mexico. The experiment consisted of three replications of a randomized complete block design. For the intercropping of maize and legumes, one row of legumes was planted between each row of maize. Sowing was performed using a punch stroke, with a distance of 100 cm between rows and 40 cm between plants (25,000 plants ha^{-1}). For the monocropping system, maize plants were sown with a distance of 50 cm between rows and 40 cm between plants (50,000 plants ha^{-1}). The total planted area was 3456 m^2 (Figure 1). Plant densities were 2.1 plants m^{-2} for maize and legumes and 4.2 plants m^{-2} for the maize monocropping system. The three cropping systems were as follows: (1) maize/crotalaria intercropping, (2) maize/cowpea intercropping, and (3) maize monocropping. In this model, however, only data from the maize/cowpea intercropping treatment were used. The crop row arrangement of maize and cowpea intercropping systems was 1 m of maize rows alternated with 1 m of cowpea rows (row unit: maize–cowpea–maize). All crops were planted by hand, but maize was planted first on 17 July 2021, followed by cowpea on 30 July 2021. The fertilizer application was divided into two applications: half of the nitrogen and all of the phosphorus were applied one week after the emergence of the seedlings, and the remainder of the fertilizer was applied four weeks after the first application (growth stage). No insecticides were used, and the weeding process was manual. Throughout the growing season, measurements were taken of aboveground dry matter, leaf area, and plant height. Due to a lack of data from the regional climate station, weather information was downloaded from the NASA Solar Power System [46]. Before and throughout the growing season, soil data were collected.

The code for simulating dry matter growth and development in CERES and CROPGRO was modified in the DSSAT-CSM. Equations originally developed by Pronk [48] and Gou [15] were slightly modified and integrated into the MZ_GROSUB.FOR to simulate cereal growth and PHOTO.FOR to simulate legume growth. For maize growth, daily net assimilation is estimated from the daily radiation use efficiency (RUE) and photosynthetically active radiation (*PAR*) intercepted by each crop in an intercropping system. The following equation calculates maize's daily biomass production ($PCARB_{INT}$):

$$PCARB_{INT} = \left(\frac{PAR}{PLTPOP}\right) \times f_{mz-upper} \times RUE \times PCO2 + \left(\frac{PAR}{PLTPOP}\right) \times f_{mz-lower} \times RUE \times PCO2 \tag{25}$$

where RUE is radiation use efficiency (g MJ^{-1} *PAR*), *PAR* is the photosynthetically active radiation for both crop species, and daily solar radiation input is converted to *PAR* [49]. PAR/SR = 0.5 [13] was used to estimate the PAR. $f_{mz-upper}$ is the fraction of light intercepted in the upper layer of maize and $f_{mz-lower}$ is the fraction of light intercepted in the lower part of maize. RUE for a vegetative stage is defined as the ratio of total dry matter to intercepted PAR (g MJ^{-1} PAR).

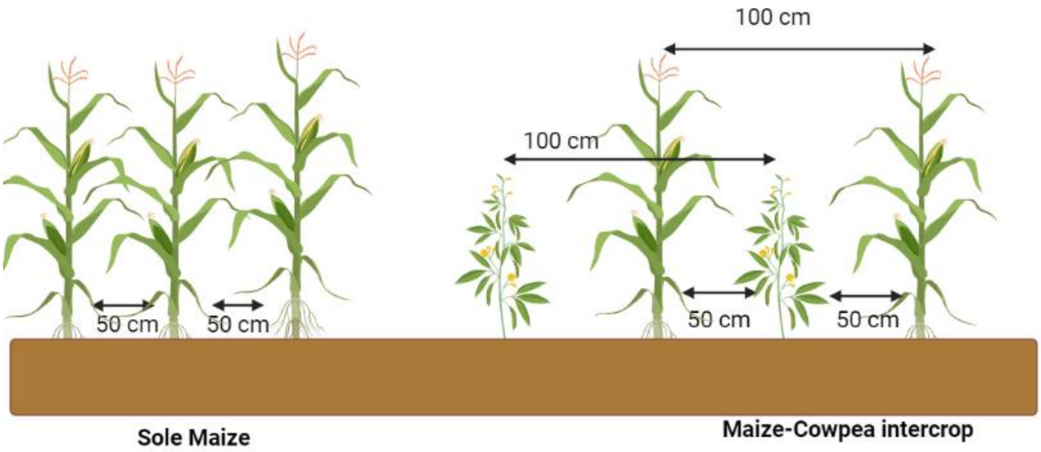

Figure 1. Schematic diagram indicating the different planting patterns. Created in biorender.com, [47] accessed on 20 February 2023.

To estimate legume growth, the same approach as in the CROPGRO model was used. The second option calculates light interception and photosynthesis on an hourly basis [50]. After calculating gross photosynthesis and daily maintenance respiration, the model estimates potential carbon partitioning to both vegetative and reproductive structures. However, the daily gross photosynthesis (PG), where PGFAC is the multiplier to compute daily canopy PG as a function of LAI, was substituted by a lower and an upper layer of the shorter crop (Equation (24)). When the legume is grown as a strip in phases I or V, Equation (1) is used to calculate the fraction of light intercepted. In phases II and IV, Equations (12) and (24) are used to calculate the fraction of light intercepted by the legume species. In phase III, in the case of intercropping species with equal heights, the fraction of radiation intercepted by each plant strip is calculated according to Equations (12)–(22) as used for phases II and IV, but with $IP = IR = 1$ for both species, and $SP = 1$.

2.4. MPI_DSSAT Model Scenario Setting Assessment

This integrated model was primarily designed to simulate the interspecific competition between cereal–legume intercropping systems. To capture the ability of the DSSAT intercrop model, we used a few hypothetical scenarios to test the model's effects on LAI, biomass production, and grain yield. The following scenarios were performed: (1) maize monocrop with a double plant population compared to maize intercropped with maize, with the same planting dates; (2) cowpea monocrop with double the plant population compared to cowpea intercropped with itself, with the same planting dates; and (3) maize intercropped with cowpea, with the same planting dates and different planting dates.

2.5. Capturing the Light Competition Performance in the Model

Three hypothetical tests were used to evaluate the performance of the model in a light competition. We assumed that neither water nor nitrogen was limited for all tests. Taking row spacing and plant population density into account, a maize monocrop experiment was designed with double the plant population of one intercropped with maize. In the first scenario, the yield potential of the maize monocrop versus the maize intercrop was evaluated (Figure 2). The maize monocrop with a plant population density of 4.2 plants m^{-2} and a row spacing of 80 cm was compared to maize intercropped with maize with a plant population density of 2.1 plants m^{-2} and a row spacing of 40 cm. All plants in both cropping systems were planted on the same day.

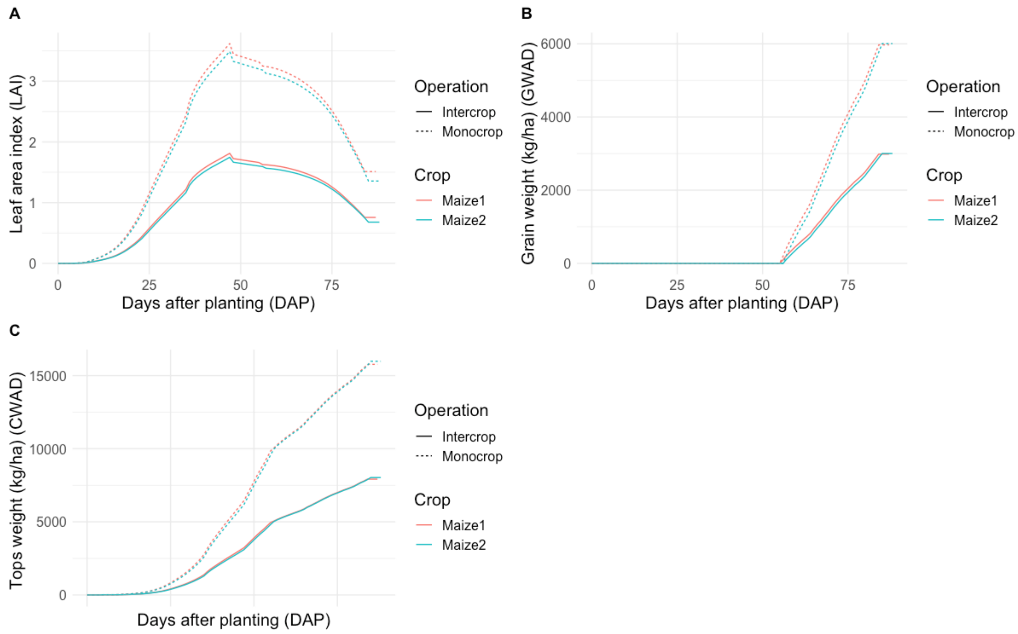

Figure 2. Potential run of maize monocrop versus maize intercropped with maize: (**A**) LAI is leaf area index; (**B**) GWAD is total grain weight); (**C**) CWAD is total top weight.

3. Results and Discussion

The results indicated that the intercrop model was able to simulate similar LAI (Figure 2A), grain yield (Figure 2B), and dry matter production (Figure 2C) when compared to a maize monocrop with double the plant population (Table A1, Appendix A). This shows that our method for simulating light competition in the intercrop model is effective. In the second scenario, the yield potential of a cowpea monocrop versus cowpea intercrop was evaluated (Figure 3). Similar results (Figure 3A–C) were observed when the cowpea monocrop was compared with the cowpea intercrop with the same planting dates, row spacing, and plant population density used in the previous hypothetical experiment (Figure 1). In either the first or second scenario, the slight difference in result variation was caused by a small alteration made to the cultivar coefficient so that both lines of the graph could be observed. Overall, this demonstrates that our method for simulating light competition in the model is effective. A similar light interception algorithm has been implemented in numerous intercrop models [50,51].

In the third scenario, the yield potential of a maize monocrop was compared to a maize–cowpea intercrop (Figure 4). The yield potential of the maize monocrop was evaluated using data from sole maize and maize–cowpea intercropping systems, with total dry matter of maize data taken between 65 and 85 days after the maize sowing date and 35 days after physiological maturity for maize grain yield. Data for the cowpea monocrop were not collected. Because of that, it was not important to run any statistics such as the correlation-based statistics, i.e., the coefficient of determination (R^2), the root mean square error (RMSE), and the index of agreement (D-index), to validate this model. So, it was not possible to compare the measured and simulated values of cowpea in this model. In the maize monocrop, a plant population density of 4.2 plants m^{-2} with a row spacing of 50 cm was used. In the maize–cowpea intercropping system, both crop species were planted at a plant population density of 2.1 plants m^{-2}, with a row spacing of 100 cm. In this experiment, we simulated maize crops in both systems (i.e., monocropping and intercropping systems), as well as sole cowpea crops planted on the same day and cowpea crops in the intercropping system planted 15 days after maize. Our results indicate that the intercrop model reasonably simulated the grain yield (Figure 4B) and dry matter production (Figure 4C) of maize. Our results are similar to the study conducted by Chimonyo et al. [52], in which they evaluated a sorghum–cowpea intercrop system using the APSIM model and found it capable of simulating growth and yield, but with a slight overestimation of biomass (6.25%) and yield (14.93%). However, no data on LAI were taken for this experiment, so the results presented here are hypothetical (Figure 4A). This shows that our method for simulating light competition in the maize–cowpea intercrop model is promising. The intercrop model reasonably simulated the dry matter production of cowpea; however, no data were taken regarding LAI or grain yield. The capability of the model to distribute radiation across the canopy of a maize–cowpea intercrop was demonstrated to be a useful strategy in accurately simulating the accumulation of biomass within the intercrop, highlighting the importance of this approach in intercropping research. Therefore, due to its capability of efficiently allocating resources within diverse crop stands, the newly developed MPI_DSSAT Model is a valuable approach for analyzing resource utilization in intercropping systems. While Alderman [53] tested the MPI approach for parallelizing simulations using DSSAT-CSM, and Fernandes et al. [54] tested it for integrating a crop model and pest/disease models using DSSAT-CSM, our study can be considered the first to use the MPI approach for simulating light interception in intercropping systems. Additionally, Kang et al. [55] previously created an MPI parallel method for the EPIC model, an agroecosystem model used in global food and bioenergy studies. The MPI_coupling interface presented in this study is a versatile solution that can be applied to any model written in a language with MPI bindings, such as C, C^{++}, and FORTRAN (i.e., Formula Translation, computer programming language (Fernandes et al. [54]). Furthermore, this technique is compatible with programming languages that can interface with MPI libraries, including popular languages such as R and Python, which are widely used by data scientists (Fernandes et al. [54]). Therefore, the MPI_coupling interface has the potential to significantly enhance the performance of a broad range of models and simulations. Finally, in the hypothetical results, we observed a big reduction in the performance of the intercrop model. This might be due to the strip width (R) and path width (P) values used in the model. Therefore, we suggest that these values be evaluated and changed in the light competition equations to improve the model's performance.

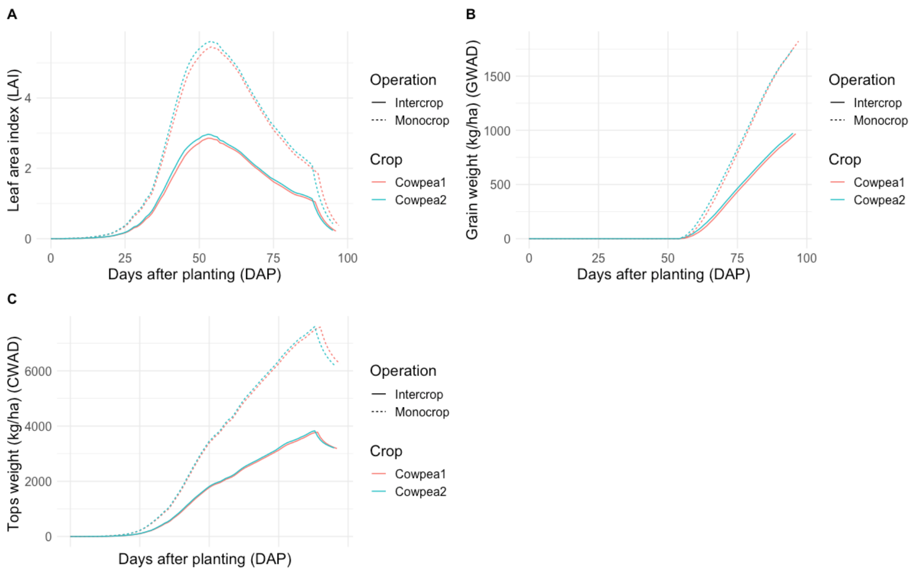

Figure 3. Potential run of cowpea monocrop versus cowpea intercropped with cowpea: (**A**) LAI is leaf area index; (**B**) GWAD is total grain weight); (**C**) CWAD is total top weight.

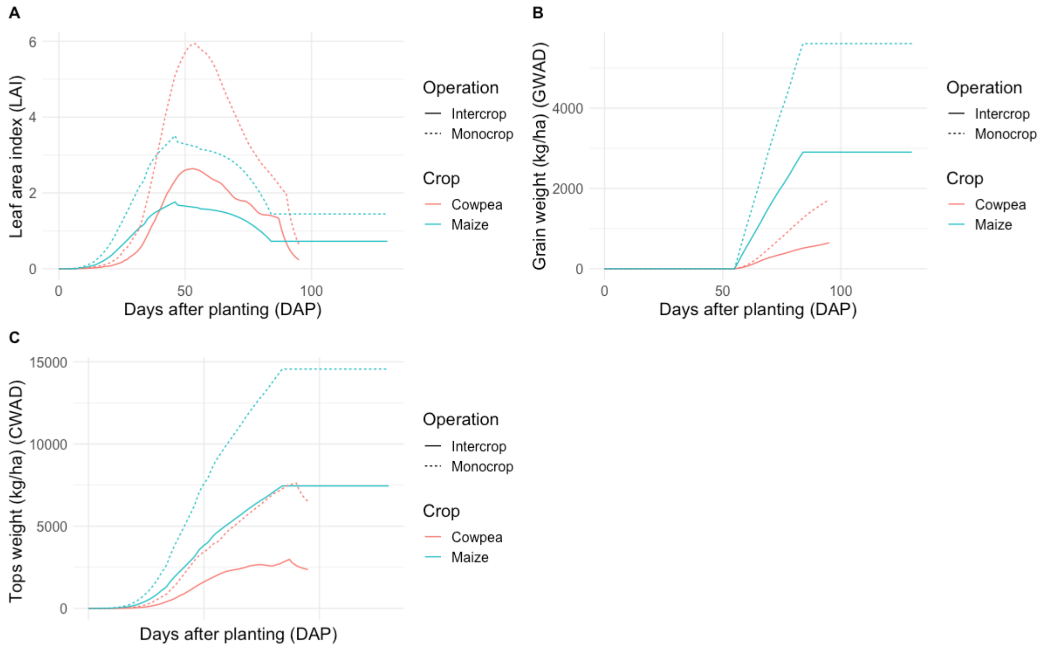

Figure 4. Potential run of maize monocrop versus maize intercropped with cowpea: (**A**) CWAD is total dry matter production; (**B**) GWAD is total grain yield; (**C**) LAI is leaf area index.

4. Conclusions

To advance the capabilities of DSSAT for allowing intercropping systems, we used the MPI parallelization technique and applied it to the MPI_DSSAT intercropping model. The first part of the model was developed as a deterministic model. A case study was conducted to test the capacity of the MPI_DSSAT intercrop model to perform maize–legume simulations using data from a field experiment conducted in Becal, Campeche, Mexico. However, these data are not sufficient to validate the model. Several field experiments from different environments are currently being conducted to validate this model before releasing it for fieldwork by the scientific community. As the data for this model came from a single site with three replications, no statistical analysis, i.e., coefficient of determination (R2), root mean square error (RMSE), or the index of agreement (D-index), was used to validate it. The results show that the MPI_DSSAT intercrop model is capable of serving a valuable role in exploring production and management scenarios in maize–legume intercropping systems. For example, in this study, the MPI_DSSAT intercrop modeling platform seems promising in its ability to predict maize yield and dry matter production (Table A1, Appendix A). Nevertheless, it was not possible to compare the observed and simulated values of cowpea crops in this model due to the absence of data. While this study targets maize–cowpea intercropping systems, this model is a generic one that can easily be used as a template for any cereal and non-cereal intercropping model within DSSAT. Some code in the MPI_DSSAT intercrop model associated with different module versions and light interception algorithm platforms may need to be adjusted and improved. Additionally, detailed model input data and experiment data for calibration and validation are other challenges that limit reliable regional and global application.

Author Contributions: Conceptualization, J.F.P. and U.S.; methodology, W.P.; software, W.P.; validation, W.P., U.S. and J.F.P.; formal analysis, U.S..; investigation, J.F.P.; resources, E.R.-S.; data curation, J.F.P.; writing—original draft preparation, J.F.P.; writing—review and editing, W.P.; visualization, W.P.; supervision, U.S.; project administration, E.R.-S.; funding acquisition, U.S. All authors have read and agreed to the published version of the manuscript.

Funding: This research received no external funding. The Article Processing Charges (APC) was funded by the International Fertilizer Development Center (IFDC).

Institutional Review Board Statement: Not applicable.

Data Availability Statement: The data presented in this study are available on request from the corresponding author.

Acknowledgments: The authors thank the National Council for Science and Technology (CONACYT) for their financial support through a scholarship to Jacques Fils Pierre. Thanks also to IFDC, University of Kentucky and University of Wisconsin-Madison for their training during the development of this model. Special thanks to Julie Kohler for the extensive English revisions.

Conflicts of Interest: The authors declare no conflict of interest.

Appendix A

Table A1. Mean observed and simulated values for grain and dry matter yield of maize under different cropping systems.

Treatment	Mean (Obs.)	Mean (Sim.)	Mean (Obs.)	Mean (Sim.)
	Grain yield (kg ha^{-1})		Dry matter yield (kg ha^{-1})	
Maize–Cowpea	3991	2905	10,476	7451
Sole Maize	5285	5608	11,145	14,555

References

1. Addo-Quaye, A.A.; Darkwa, A.A.; Ocloo, G.K. Yield and productivity of component crops in a maize-soybean intercropping system as affected by time of planting and spatial arrangement. *J. Agric. Biol. Sci.* **2011**, *6*, 50–57.
2. Akande, M.O.; Oluwatoyinbo, F.I.; Kayode, C.O.; Olowokere, F.A. Response of Maize (*Zea mays*) and Okra (Abelmoschus esculentus) Intercrop Relayed with Cowpea (Vigna unguiculata) to Different Levels of Cow Dung Amended Phosphate Rock. *World J. Agric. Sci.* **2006**, *2*, 119–122.
3. Ball, D.; Shaffer, M.J. Simulating resource competition in multispecies agricultural plant communities. *Weed Res.* **1993**, *33*, 299–310. [CrossRef]
4. Baumann, D.; Bastiaans, L.; Goudriaan, J.; van Laar, H.; Kropff, M. Analysing crop yield and plant quality in an intercropping system using an eco-physiological model for interplant competition. *Agric. Syst.* **2002**, *73*, 173–203. [CrossRef]
5. Berghuijs, H.N.C.; Wang, Z.; Stomph, T.J.; Weih, M.; Van Der Werf, W.; Vico, G. Identification of species traits enhancing yield in wheat-faba bean intercropping: Development and sensitivity analysis of a minimalist mixture model. *Plant Soil* **2020**, *455*, 203–226. [CrossRef]
6. Berntsen, J.; Hauggard-Nielsen, H.; Olesen, J.; Petersen, B.; Jensen, E.; Thomsen, A. Modelling dry matter production and resource use in intercrops of pea and barley. *Field Crop. Res.* **2004**, *88*, 69–83. [CrossRef]
7. Biedrzycki, M.L.; Jilany, T.A.; Dudley, S.A.; Bais, H.P. Root exudates mediate kin recognition in plants. *Commun. Integr. Biol.* **2010**, *3*, 28–35. [CrossRef]
8. Boote, K.; Pickering, N. Modeling Photosynthesis of Row Crop Canopies. *Hortscience* **1994**, *29*, 1423–1434. [CrossRef]
9. Brooker, R.W.; Bennett, A.E.; Cong, W.-F.; Daniell, T.J.; George, T.S.; Hallett, P.D.; Hawes, C.; Iannetta, P.P.M.; Jones, H.G.; Karley, A.J.; et al. Improving intercropping: A synthesis of research in agronomy, plant physiology and ecology. *New Phytol.* **2015**, *206*, 107–117. [CrossRef]
10. Caldwell, R.M. *Simulation Models for Intercropping Systems*; Sinoquet, H., Cruz, P., Eds.; INRA editions; Ecophysiology of tropical intercropping, Institut National de la Recherche Agronomique: Paris, France, 1995; pp. 353–368.
11. Chamkhi, I.; Cheto, S.; Geistlinger, J.; Zeroual, Y.; Kouisni, L.; Bargaz, A.; Ghoulam, C. Legume-based intercropping systems promote beneficial rhizobacterial community and crop yield under stressing conditions. *Ind. Crop. Prod.* **2022**, *183*, 114958. [CrossRef]
12. Cvitanovic, C.; Hobday, A.J.; van Kerkhoff, L.; Wilson, S.K.; Dobbs, K.; Marshall, N.A. Improving knowledge exchange among scientists and decision-makers to facilitate the adaptive governance of marine resources: A review of knowledge and research needs. *Ocean Coast. Manag.* **2015**, *112*, 25–35. [CrossRef]
13. Feike, T.; Pfenning, J.; Graeff-Hönninger, S.; Chen, Q.; Claupein, W. Adaptation of CROPGRO to Chinese cabbage I. Estimation of cardinal temperatures. In *Grasping the Complexity of Intercropping—Developing and Testing an Integrated Decision Support System for Vegetable Production in the North China Plain*; University of Hohenheim: Stuttgart, Germany, 2010.
14. Hoogenboom, G.; Porter, C.H.; Boote, K.J.; Shelia, V.; Wilkens, P.W.; Singh, U.; White, J.W.; Asseng, S.; Lizaso, J.I.; Moreno, L.P.; et al. The DSSAT crop modeling ecosystem. In *Advances in Crop Modeling for a Sustainable Agriculture*; Boote, K.J., Ed.; Burleigh Dodds Science Publishing: Cambridge, UK, 2019; pp. 173–216. [CrossRef]
15. Gao, Y.; Duan, A.; Qiu, X.; Sun, J.; Zhang, J.; Liu, H.; Wang, H. Distribution and Use Efficiency of Photosynthetically Active Radiation in Strip Intercropping of Maize and Soybean. *Agron. J.* **2010**, *102*, 1149–1157. [CrossRef]
16. Gao, Y.; Duan, A.; Qiu, X.; Liu, Z.; Sun, J.; Zhang, J.; Wang, H. Distribution of roots and root length density in a maize/soybean strip intercropping system. *Agric. Water Manag.* **2010**, *98*, 199–212. [CrossRef]

17. Gou, F. On Yield Gains and Yield Gaps in Wheat-Maize Intercropping: Opportunities for Sustainable Increases in Grain Production. Ph.D. Thesis, Wageningen University, Wageningen, The Netherlands, 2017. [CrossRef]
18. Goudriaan, J. Crop Micrometeorology: A Simulation Study. In *Simulation Monographs*; Pudoc: Wageningen, The Netherlands, 1977.
19. Gruntman, M.; Groß, D.; Májeková, M.; Tielbörger, K. Decision-making in plants under competition. *Nat. Commun.* **2017**, *8*, 2235. [CrossRef]
20. Hoogenboom, G.; Porter, C.H.; Shelia, V.; Boote, K.J.; Singh, U.; White, J.W.; Hunt, L.A.; Ogoshi, R.; Lizaso, J.I.; Koo, J.; et al. *Decision Support System for Agrotechnology Transfer (DSSAT), Version 4.7*; DSSAT Foundation: Gainesville, FL, USA, 2019; Available online: www.DSSAT.net (accessed on 26 October 2021).
21. Hoogenboom, G.; Jones, J.W.; Traore, P.C.S.; Boote, K.J. Experiments and data for model evaluation and application. In *Improving Soil Fertility Recommendations in Africa Using the Decision Support System for Agrotechnology Transfers (DSSAT)*; Kihara, J., Fatondji, D., Jones, J.W., Hoogenboom, G., Tabo, R., Bationo, A., Eds.; Springer: Dordrecht, The Netherlands, 2012; pp. 9–18.
22. Jensen, E.S.; Carlsson, G.; Hauggaard-Nielsen, H. Intercropping of grain legumes and cereals improves the use of soil N resources and reduces the requirement for synthetic fertilizer N: A global-scale analysis. *Agron. Sustain. Dev.* **2020**, *40*, 5. [CrossRef]
23. Jones, C.A.; Kiniry, J.R. *CERES-Maize: A Simulation Model of Maize Growth and Development*; Texas A&M Univ. Press: College Station, TX, USA, 1986.
24. Jones, J.W.; Hoogenboom, G.; Porter, C.H.; Boote, K.J.; Batchelor, W.D.; Hunt, L.A.; Wilkens, P.W.; Singh, U.; Gijsman, A.J.; Ritchie, J.T. The DSSAT cropping system model. *Eur. J. Agron.* **2003**, *18*, 235–265. [CrossRef]
25. Keating, B.; Carberry, P. Resource capture and use in intercropping: Solar radiation. *Field Crop. Res.* **1993**, *34*, 273–301. [CrossRef]
26. Keating, B.A.; Carberry, P.S.; Hammer, G.L.; Probert, M.E.; Robertson, M.J.; Holzworth, D.; Huth, N.I.; Hargreaves, J.N.; Meinke, H.; Hochman, Z.; et al. An overview of APSIM, a model designed for farming systems simulation. *Eur. J. Agron.* **2003**, *18*, 267–288. [CrossRef]
27. Knörzer, H.; Grae-Hönninger, S.; Müller, B.U.; Piepho, H.-P.; Claupein, W. A modeling approach to simulate effects of intercropping and interspecific competition in arable crops. *Int. J. Inf. Syst. Soc. Change* **2010**, *1*, 44–65. [CrossRef]
28. Kropff, M.J.; Vossen, F.J.H.; Spitters, C.J.T.; De Groot, W. Competition between a maize crop and a natural population of *Echinochloa crus-galli* (L.) PB Neth. *J. Agric. Sci.* **1984**, *32*, 324–327.
29. Kropff, M.J.; van Laar, H.H. *Modelling Crop-Weed Interactions*; CAB International: Wallingford, UK; International Rice Research Institute: Los Baños, Philippines, 1993.
30. Lantinga, E.A.; Nassiri, M.; Kropff, M.J. Modelling and measuring vertical light absorption within grass–clover mixtures. *Agric. For. Meteorol.* **1999**, *96*, 71–83. [CrossRef]
31. Li, L.; Sun, J.; Zhang, F.; Guo, T.; Bao, X.; Smith, F.A.; Smith, S.E. Root distribution and interactions between intercropped species. *Oecologia* **2005**, *147*, 280–290. [CrossRef] [PubMed]
32. Liu, X.; Rahman, T.; Yang, F.; Song, C.; Yong, T.; Liu, J.; Zhang, C.; Yang, W. PAR Interception and Utilization in Different Maize and Soybean Intercropping Patterns. *PLoS ONE* **2017**, *12*, e0169218. [CrossRef] [PubMed]
33. Lizaso, J.I.; Boote, K.J.; Jones, J.W.; Porter, C.H.; Echarte, L.; Westgate, M.E.; Sonohat, G. CSM-IXIM: A New Maize Simulation Model for DSSAT Version 4.5. *Agron. J.* **2011**, *103*, 766–779. [CrossRef]
34. Loomis, R.S.; Williams, W.M. Maximum crop productivity: An estimate. *Crop Sci.* **1963**, *3*, 67–72. [CrossRef]
35. Lulie, B. Intercropping Practice as an Alternative Pathway for Sustainable Agriculture: A Review. *Acad. Res. J. Agric. Sci. Res.* **2017**, *5*, 440–452. [CrossRef]
36. Mahallati, M.N.; Koocheki, A.; Mondani, F.; Feizi, H.; Amirmoradi, S. Determination of optimal strip width in strip intercropping of maize (*Zea mays* L.) and bean (*Phaseolus vulgaris* L.) in Northeast Iran. *J. Clean. Prod.* **2015**, *106*, 343–350. [CrossRef]
37. McErlich, A.F.; Boydston, R.A. Current State of Weed Management in Organic and Conventional Cropping Systems. In *Automation: The Future of Weed Control in Cropping Systems*; Springer: Dordrecht, The Netherlands, 2014; pp. 11–32. Available online: https://digitalcommons.unl.edu/cgi/viewcontent.cgi?article=2392&context=usdaarsfacpub (accessed on 26 October 2021).
38. Monteith, J.L. Climate and the efficiency of crop production in Britain. *Philos. Trans. R. Soc. B* **1977**, *281*, 277–294. [CrossRef]
39. NASA. NASA-Agroclimatology Methodology. 2012. Available online: https://power.larc.nasa.gov/data-access-viewer/ (accessed on 24 April 2022).
40. Nelson, W.; Hoffmann, M.; Vadez, V.; Roetter, R.; Whitbread, A. Testing pearl millet and cowpea intercropping systems under high temperatures. *Field Crop. Res.* **2018**, *217*, 150–166. [CrossRef]
41. Ninkovic, V.; Rensing, M.; Dahlin, I.; Markovic, D. Who is my neighbor? Volatile cues in plant interactions. *Plant Signal. Behav.* **2019**, *14*, 1634993. [CrossRef]
42. Ofori, F.; Stern, W.R. Cereal–legume intercropping systems. *Adv. Agron.* **1987**, *41*, 41–90.
43. Pierre, J.F.; Latournerie-Moreno, L.; Garruña-Hernández, R.; Jacobsen, K.L.; Laboski, C.A.M.; Salazar-Barrientos, L.d.L.; Ruiz-Sánchez, E. Farmer Perceptions of Adopting Novel Legumes in Traditional Maize-Based Farming Systems in the Yucatan Peninsula. *Sustainability* **2021**, *13*, 11503. [CrossRef]
44. Punyalue, A.; Jamjod, S.; Rerkasem, B. Intercropping maize with legumes for sustainable highland maize production. *Mt. Res. Dev.* **2018**, *38*, 35–44. Available online: https://bioone.org/journals/mountain-research-and-development/volume-38/issue-1/MRD-JOURNAL-D-17-00048.1/Intercropping-Maize-With-Legumes-for-Sustainable-Highland-Maize-Production/10.1659/MRD-JOURNAL-D-17-00048.1.full (accessed on 26 October 2021). [CrossRef]

45. Rapholo, E.; Odhiambo, J.J.O.; Nelson, W.C.D.; Rötter, R.P.; Ayisi, K.; Koch, M.; Hoffmann, M.P. Maize–lablab intercropping is promising in supporting the sustainable intensification of smallholder cropping systems under high climate risk in Southern Africa. *Exp. Agric.* **2019**, *56*, 104–117. [CrossRef]
46. Ritchie, J.T.; Otter, S. Description and performance of CERES-Wheat: A user-oriented wheat yield model. In *ARS Wheat Yield Project*; Willis, W.O., Ed.; ARS-38; National Technical Information Services: Springfield, VA, USA, 1985; pp. 159–175.
47. BioRender.com. 2022. Available online: https://app.biorender.com/illustrations/621d6a79bfac11004c807d52 (accessed on 14 March 2022).
48. Pronk, A.A.; Goudriaan, J.; Stilma, E.; Challa, H. A simple method to estimate radiation interception by nursery stock conifers: A case study of eastern white cedar. *Neth. J. Agric. Sci.* **2003**, *51*, 279–295. [CrossRef]
49. Tsubo, M.; Walker, S.; Mukhala, E. Comparisons of radiation use efficiency of mono-/inter-cropping systems with different row orientations. *Field Crops Res.* **2001**, *71*, 17–29. [CrossRef]
50. Tsubo, M.; Walker, S. A model of radiation interception and use by a maize–bean intercrop canopy. *Agric. For. Meteorol.* **2002**, *110*, 203–215. [CrossRef]
51. Sinclair, T.R.; Gardner, F.P. *Principles of Ecology in Plant Production*; CAB International: Wallingford, UK, 1998.
52. Chimonyo, V.G.P.; Modi, A.T.; Mabhaudhi, T. Simulating yield and water use of a sorghum–cowpea intercrop using APSIM. *Agric. Water Manag.* **2016**, *177*, 317–328. [CrossRef]
53. Alderman, P.D. Parallel gridded simulation framework for DSSAT-CSM (version 4.7.5.21) using MPI and NetCDF. *Geosci. Model Dev.* **2021**, *14*, 6541–6569. [CrossRef]
54. Fernandes, J.M.; Pavan, W.; Pequeno, D.; Wiest, R.; Holbig, C.A.; Oliveira, F.; Hoogenboom, G. Improving crop pest/disease modeling. In *Advances in Crop Modeling for a Sustainable Agriculture*; Boote, K.J., Ed.; Burleigh Dodds Science Publishing: Cambridge, UK. [CrossRef]
55. Kang, S.; Wang, D.; Nichols, J.; Schuchart, J.; Kline, K.; Wei, Y.; Ricciuto, D.; Wullschleger, S.; Post, W.; Izaurralde, R. Development of mpi_EPIC model for global agroecosystem modeling. *Comput. Electron. Agric.* **2015**, *111*, 48–54. [CrossRef]